Fundamental Journals
International Journal of Fundamental Physical Sciences (IJFPS) ISSN:2231-8186
IJFPS, Vol 4, No 1, pp 26-36, March , 2014 *S.N.Hoseinimotlagh*
DOI:10.14331/ijfps.2014.330063
http://dx.doi.org/10.14331/ijfps.2014.330063

Dynamical Study on the Ultra-Short Pulsed Laser in the Water Medium and Skin Tissue and Comparing Obtained Results

S.N.Hoseinimotlagh[1], M.S.Sharifi[2], Kh.Shoja[3]

[1]Department of Physics, Islamic Azad University, Shiraz branch, Shiraz, Iran
[2]Teacher of Education Office, Fars, Sepidan, Iran
[3]Department of Physics, Islamic Azad University, Science and Research Branch, Fars, Iran

Email: hoseinimotlagh@ hotmail.com

(*Received Feb 2014; Published March 2014*)

ABSTRACT

Interest on the ultra-short laser has increased continually over the past decade. Scientists have an excellent power medical resource and the use of this resource will assist in the development of sustainable medical procedures. Scientists with its many technologies and significant medical range-might be expected to have considerable potential for treatment skin cancer. In this paper influences of the critical electron density and radiation intensity on the free-electron density for the ablation on the epidermis and dermis tissues are investigated. Our research work show existing of an inverse relationship between intensity radiations of laser pulsed and distance of focal spot with time dependent of free-electron density. This case is proper for skin cancer treatment. Also, our calculations for each medium (water and skin tissue)show that optimum time dependent free electron density for dermis layer at angle 16˚ and 22˚ which is a function of wavelength, beam width, beam radius, amplitude of the beam radiation strength and pulse duration is more than for epidermis layer.

Keywords: laser, plasma, electron, ultra short

DOI:10.14331/ijfps.2014.330063

INTRODUCTION

Since the invention of laser in 1960, a great number of potential fields for laser application have been explored. Among these applications, various kinds of laser clinical therapies have already become irreplaceable tools of modern medicine. In the early times, use of a laser to irradiate animals and eventually people showed accelerated wound healing(Mester, Spiry, Szende, & Tota, 1971; Tata & Waynant, 2011). Laser systems can be classified as continuous wave (CW) lasers and pulsed lasers. The great progress in laser treatment in clinical applications is primarily attributed to the rapid development of pulsed laser systems. Ultrafast lasers output ultra-short pulses with pulse widths ranging from picoseconds down to femtosecond. Short-pulse lasers have become greatly important in recent years for many technologies, including micro fabrication, thin-film formation, laser cleaning, and medical and biological applications. For example, short-pulse lasers are powerful tools for surface patterning and micromachining because of the noncontact nature of processing (Nieto, Flores-Arias, O'Connor, & Gómez-Reino, 2011). Pulse lasers are also widely used in medical and biological fields, e.g., laser lithotripsy, microsurgery, and dentistry, in addition to materials processing (Nieto et al., 2011). Rapid progress in laser technology has brought anew set of opportunities and challenges in the past few years with the development of high-intensity femtosecond-pulse lasers. with their relatively long-pulse counterparts, ultra short-pulse lasers have many advantages for laser material processing, including negligible heat diffusion effects, absence of the liquid phase during material removal, minimal plasma absorption and shielding effects, and smaller laser fluencies for processing, which make them capable of producing high-quality features with

high spatial resolution. Two mechanisms, multi photon absorption and avalanche ionization, also called cascade or impact ionization, are responsible for laser-induced optical breakdown. Avalanche ionization is initiated when free electrons that are present in the material absorb the laser energy through inverse bremsstrahlung absorption. During inverse bremsstrahlung absorption, seed electrons absorb laser photons by favourable collisions with heavier particles, i.e., molecules and ions. If they sustain enough favourable collisions, they will eventually gain sufficient energy to ionize other molecules on impact, freeing new electrons to repeat the process, which results in a geometric increase in the free-electron density. The plasma-mediated ablation model has been employed to explain the optical breakdown phenomenon in the visible and near-infrared wavelength region, in which plasma induced by the strong electromagnetic field of a short laser pulse without significant light absorption, is considered as the cause of breakdown. In contrast, pulsed laser ablation is the process of material removal after the target is irradiated by intensive laser pulses (Jian Jiao, 2011). Plasma formation is characterized by the growth of plasmas. Scientists (Docchio, Regondi, Capon, & Mellerio, 1988)assumed the "moving breakdown" model to analyze plasma starting times and the temporal and spatial dynamics of plasma expansion in liquids subject to nanosecond laser pulse irradiation. Also scientists (Docchio et al., 1988; Fan, 2003) modified the model by taking into account the pulse propagation to characterize the time and space dependent breakdown region induced by femtosecond laser pulses. Zhou group (Zhou, Chen, & Zhang, 2008) used the rate equation to investigate the kinetic progression of plasma in pure water generated by focused short laser pulses. Guo's group is well known in developing multi-dimensional ultra fast radiative transfer methods including the transient discrete ordinates method (Guo & Kumar, 2002; Kumar, 2001), the transient Monte Carlo method (Guo, Kumar, & San, 2000), and the transient radiation element method(Kumar, 2001). Guo's group (Guo & Kumar, 2002) also conducted experimental measurements to validate the modelling. Recently, Huang's group investigated plasma-induced ablation (H. Huang & Guo, 2010; K. Huang, Guo, & Xu, 2009) as well as thermal interaction (Jian Jiao & Guo, 2009) of focused short laser pulses with skin tissues. It is now acknowledged that pulses with very short durations, such as picosecond or femtosecond, are advantageous in many applications. Due to the extremely short pulse duration which is much shorter than the thermal relaxation time of many materials, laser interaction with materials occurs before heat diffusion ever takes place, leading to increased local temperature rise in a very short time period and minimization of heat-affecting zone. This will lessen thermal damage to the surroundings. With the use of an ultrafast pulsed laser, significant improvement in the damage localization over continuous wave and general pulsed lasers has been attained (Guo & Kumar, 2002). Then the ablation of skin tissue and water medium with Pico and femtosecond laser pulses is investigated. In this paper we discussed the interaction fundamentals between ultra-short laser with skin tissue and water medium. The two model skin tissue and water medium is an axisymmetric cylinder and are stratified as three layers with different optical properties similar to human skin tissues-epidermis, dermis, and subcutaneous fat, respectively. The ultra- short laser pulse is converged inside the skin tissue and water medium to induce plasma breakdown for ablating cancerous tissue. The intensity of the focused beam is calculated by the Beer-Lambert law, and the time-dependent free-electron density is obtained according to fourth-order Runge-Kuttamethod. Various ionization mechanisms such as chromophore is calculated to show effects on the tissue layers. In this model, the temporal evolution of free electrons (i.e. plasmas) is predicted by a rate equation. The temporal evolution of the free-electron density is also illustrated at different locations inside the skin tissue and water medium. Finally, we conclude that of the influences of the free electron density rate equation and the chromophore ionization rate, beam radius, amplitude of the beam radiation strength on the ablation inhuman skin and water medium.

MATHEMATICAL FORMULATION

Time-dependent equation of radiative transfer (ERT)

Consider a converging short laser pulse upon a biological tissue cylinder is sketched in Figure.1 (Jian Jiao, 2011). The laser beam radiation heat transfer is described by the time-dependent ERT in the cylindrical coordinate system as where μ_l,η_l, ξ_l are the three directional cosines for the discrete direction $\hat{s}^l$ is the radiative source term (the superscript$l$ is the index of discrete directions), c is the speed of light in medium, I is the radiation intensity, σ_e is the extinction coefficient that is the sum of the absorption coefficient σ_a and the scattering coefficient σ_s, t is the time (Kim & Guo, 2004).

$$\frac{1}{C}\frac{\partial I_l^d}{\partial t}+\frac{\mu_l}{r}\frac{\partial}{\partial r}\left(rI_l^d\right)-\frac{1}{r}\frac{\partial}{\partial \varphi}\left(\eta_l I_l^d\right)+\xi_l\frac{\partial I_l^d}{\partial z}+\sigma_e I_l^d=\sigma_e S_l l \quad =1,2,\dots,N \tag{1}$$

Once the intensity field is obtained, the incident radiation is calculated as (Kim & Guo, 2004; Kumar, 2001)

$$G=\sum_{l=1}^{N}\omega_l I_l^d+I^b \tag{2}$$

The incident radiation is the total intensity impinging on a point from all 0 ballistic laser irradiance I^b.The radiation intensity has two components: the ballisticcomponent I^b accounting for the incident laser beam and the diffuse component I^d standing for the scattering component of the laser beam. The ballistic component of a laser beam is expressed as (Jian Jiao & Guo, 2009; Kim & Guo, 2004).

$$I^b(r,z,t)=I_0(z)exp\left\{-4\,ln\,2\left[\frac{\left(t-\frac{|z-z_0|}{c\,cos\,\theta}\right)}{t_p}-2\right]^2\right\}exp\left[\frac{-2r^2}{\omega(z)^2}\right]exp\left(-\frac{\sigma_e|z-z_0|}{cos\,\theta}\right) \tag{3}$$

Where c is the speed of light in the medium; θ is the angle between the incident laser and the optical axis; $t_p$is thepulse width at half maximum; σ_e is the extinction coefficient, which is the summation of the absorption coefficient σ_a and the

scattering coefficientσ_s. The total time durationof a whole pulse is set as 4*t*p in this study, so that the peak of the pulse arrives at time 2*t*p. In our calculations we assumed that average laser power is 0.065W.The amplitude of the beam radiation strength$I_0(Z)$can be specified by equation following

$$I_0(Z)\left(\frac{W}{cm^2}\right)\frac{2P}{\pi\omega(z)^2} \quad (4)$$

Beam spot size ω is a function of axial position z, and it is characterized bybeam waist ω_0 at the focal point and at the Rayleighrange or focal region Z_R as following (Jian Jiao, 2011)

$$\omega(Z) = \omega_{0R}\left[1+\left(\frac{Z}{Z_R}\right)^2\right]^{\frac{1}{2}} \quad (5)$$

Whereω_{0R} is the beam waist at the focus; andZ_R is Rayleighlength that is calculated by

$$Z_R = \frac{n\pi\omega_{0R}{}^2}{\lambda M^2} \quad (6)$$

Where, n is the refractive index of the medium; λ the laserwavelength in free space; M^2 is the beam quality factor that is expressed as

$$M^2 = \frac{\omega_{0R}\theta_R}{\theta\omega_0} \quad (7)$$

Here, $\theta_R$is the far-field divergence of a real beam; ω_0 andθ arethe beam waist and far-field divergence of a true Gaussian beam, respectively. In our calculations we assume that M^2 = 1 for each medium (water and skin tissue)

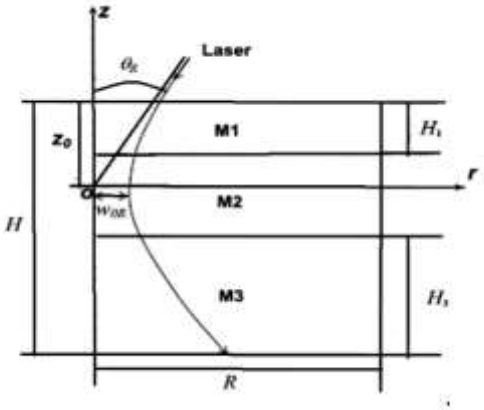

Figure.1 Sketch of the geometric coordinates and dimension (Jian Jiao, 2011)

RATE EQUATION

The general form of the rate equation of the time evolution of the free electron density is given by (Kumar, 2001).

$$\frac{\partial\rho}{\partial t} = \left(\frac{\partial\rho}{\partial t}\right)_{mp} + \left(\frac{\partial\rho}{\partial t}\right)_{ch} + \eta_{casc}\rho - g\rho - \eta_{rec}\rho^2 \quad (8)$$

Where ρ is the time dependent free-electron density. The first three terms on the right hand side represent the production of free electrons through multiphoton, chromophore and cascade (avalanche) ionizations, respectively. Last two terms are the electron losses due to diffusion and recombination, respectively. The multiphoton and cascade (avalanche) ionizations and diffusion rates are expressed as (Jian Jiao, 2011).

$$\left(\frac{\partial\rho}{\partial t}\right)_{mp} \approx$$

$$\frac{2\omega}{9\pi}\left(\frac{m'\omega}{\hbar}\right)^{\frac{3}{2}}\left[\frac{e^2}{16m'\Delta E\omega^2 cn\varepsilon_0}G\right]^k exp(2k)\varphi\left(\sqrt{2k-\frac{2\Delta E}{\hbar\omega}}\right) \quad (9)$$

$$\eta_{casc} = \frac{1}{\omega^2\tau^2+1}\left(\frac{e^2\tau}{cnm\Delta E\varepsilon_0}G - \frac{m\tau\omega^2}{M_m}\right) \quad (10)$$

$$g = \frac{\tau\Delta E}{3m}\left[\left(\frac{2.4}{\omega_{0R}}\right)^2 + \left(\frac{1}{Z_R}\right)^2\right] \quad (11)$$

The recombination rate is considered to be η_{rec} =2×10^{-9} cm^3/s (Kennedy, 1995). The ionization energy is $E = 6.5\ eV$ and $E = 4.6\ eV$ for water medium (Williams, Varma, & Hillenius, 2008) and skin tissue (Ding, Lu, Wooden, Kragel, & Hu, 2006; Fang & Hu, 2004), respectively. The second term on the right hand side Eq.(5), the quasi-free-electron density due to chromophore ionization is estimated as (Fang & Hu, 2004)

$$\rho_{ch}(t) = \frac{3\sqrt{\pi}}{4}\eta_{ch}N_b\left[\frac{2k_B}{\Delta E}\left(T_0+\frac{F(t)\mu_a}{c_{ch}u_{ch}f_{ch}}\right)\right]^{\frac{1}{2}} exp\left\{-\frac{\Delta E}{2k_B\left[T_0+\frac{F(t)\mu_a}{c_{ch}u_{ch}f_{ch}}\right]}\right\} \quad (12)$$

A necessary condition for the chromophore ionization pathway in producing quasi-free electrons lies in adiabatic heating of the chromophore by the ultra-short laser pulses. The characteristics time of thermal energy transport out of an described chromophore is proposed to be 20 μs (Fang & Hu, 2004).Therefore, the adiabatic heating condition can be assumed for the ablation induced duo to picosecond or femtosecond laser interaction within each medium. Where $F(t) = \int_0^t G(t)dt$ is the time dependent integral of the incident radiation: η_{ch}~$1\times10^{15}m^{-3}$is the number density of chromophore in skin tissue and water,$N_b \approx 1\times10^{11}$is the average number of bound electrons per chromophore, $u_{ch} = 1.35\times10^3\ kgm^{-3}$ mass density, k_B is theBoltzmann constant; T_0 is the ambient temperature assumed to be 300 K,$c_{ch} = 2.51\times10^3\ Jkg^{-1}K^{-1}$ is the specific heat of melano some organelles, $f_{ch} \approx 0.5\%$is the volume ratio of the chromophores to skin and water(Fang,2004). By taking a partial derivative f the free-electron density with respect to time, the chromophore ionization rate is calculated.

PROPERTIES OF EACH MEDIUM

In this paper, for comparing our obtained results of each two media (water and skin tissue), we are considered the common wavelengths532, 580 and 1064 nm. A constant absorption and scattering coefficients of the plasmas generated by the pulsed laser is assumed. The epidermis layer absorption coefficient is adopted as σ_{aed} = 0.02 $mm^{-1}$and for dermis is σ_{ad} = 0.05 mm^{-1}, the optical properties of the tissues for each medium at three wavelength are listed in Table 1.In this work, human skin ($H = 5mm, R = 5mm$) is organized in distinct layers and cylindrical coordinate variables are z and r. Which the high of epidermis, dermis and subcutaneous fat are, (H_e=0.5mm), (H_d=1.5mm), ($H_f = 3mm$), respectively. In this paper, the focused laser beam will incident on the surface of the epidermis and dermis layers within water and skin tissue. To induce plasma ablation in two medium, use of ultra-short pulsed (USP) lasers with pulse duration down to picoseconds

or femtosecond is required. The optical properties of the skin tissues at different wavelengths are listed in Table1. The refractive index of the skin tissues is assumed to be constant at 1.40 (Ding et al., 2006). Refractive index calculated used for water medium, is1.33.

Table1 Optical properties of the skin tissues at wavelength 1064 nm (Ding et al., 2006).

Tissue type	Epidermis	Dermis	Fat
$\sigma_a(mm^{-1})$	۰,۰۲	۰,۰۵	۰,۰۷
$\sigma_s(mm^{-1})$	۳,۰	۱,۸۳	۱,۶۹

RESULTS AND DISCUSSION

Using the presented models and available data, we consider the time dependent free electron density in water medium and skin tissue. Therefore, a laser beam is assumed to be converged to a small spot at the skin layer by a single objective lens with angle of 16 and 22 degree. Now the study on the plasma-mediated ablation is extended to the models water medium and skin tissue for different layers. A focused laser beam will incident on the surface of the epidermis or inside (dermis) in water medium and skin tissue. The focused laser beam technology is adapted to its propagation in the water medium and skin tissue is simulated via solving the kinetic equation of radiative transfer with Rung-Kutta method. In the numerical models, the optical breakdown in the water medium and skin tissue is identified when the maximum free- electron density generated at the focal spot centre during the period of one laser pulse equals to a critical electron density. In this work, we calculated the time evolution of the free-electron density in a control volume. The technique of converging beam is a non-invasive method which ideally delivers energy to a location inside the body and avoids undesirable reactions in the surrounding healthy tissues. To study on the ablation in a biological tissue, the attenuation of lights due to the absorption and scattering effects are such that needs to be accurately taken into account. Our numerical calculations for free electron density at three wavelength show that, the highest free-electron density would be occurred in the layer dermis at16 degree.

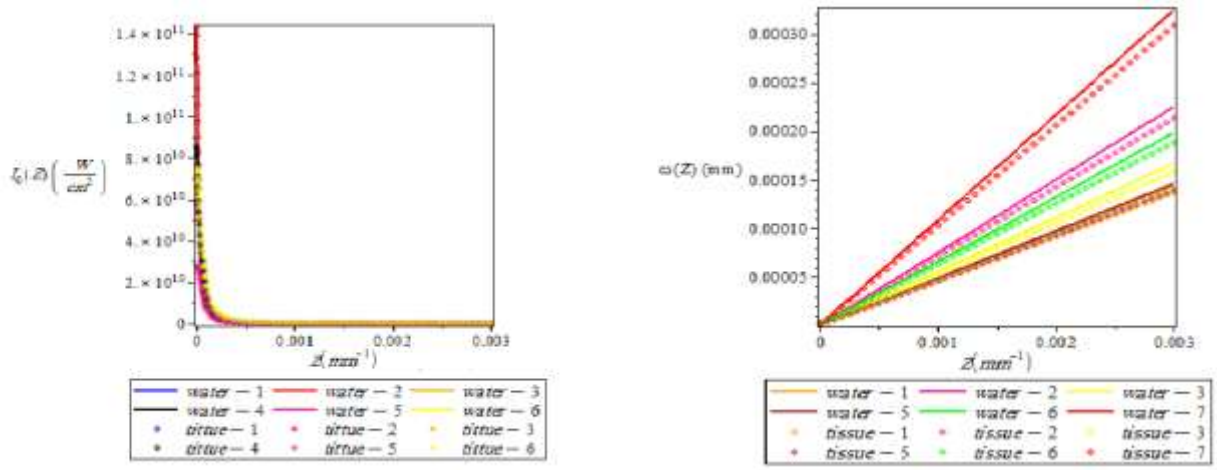

a **b**

Figure.2 Comparison of the skin tissue and water medium **a)** $I_0(z)$, ***b***)ω(z) as a functions of the $Z(mm^{-1})$

Figure 2(a) show the distance variations of ω(z) (beam radius) eq.5, for various wavelengths such as 532, 580, 1064 nm at different physical conditions that are listed in Table 2 for water medium (solid line) and skin tissue (spot line). Here we estimated ω(z) produced by laser pulse 30 ps at wavelength 1064 nm is maximum and the laser pulse 6000 ns at wavelength 532 is minimum. We find that ω(z) in the water medium much is greater than that for skin tissue, due to differences in the refractive index; hence, the Rayleigh length calculated is different. Fig. 2(b) show the distance variations of $I_0(z)$ (beam radiation strength) Eq.(4) for various wavelengths at different physical conditions that for water medium (solid line) and skin tissue (spot line). Here $I_0(z)$ calculated in the skin tissue and is more than water medium, due to differences in the refractive index and the Rayleigh length calculated, then maximum calculate $I_0(z)$ from the focusspot the incoming laser beam ($z = 0$). The maximum irradiance is always at the beam focus (J Jiao & Guo, 2011). The extinction coefficient is from the layers dermis 1.88 mm^{-1} and epidermis 3.02 mm^{-1}. As expressed in Eq.(3), the I^b is depends on the extinction coefficient, angle and layers depth counter. Our numerical calculations show that I^b in the skin tissue is much greater than water medium, due to differences in the refractive index. The Rayleigh length, beam width and $I_0(z)$ calculated. There are not differences of viewpointI^bamountbetween layers configuration for each medium in the 2-D and 3-D models. The multi photon and cascade ionizations are the primary mechanisms for the USP laser ablation on the models skin tissue and water medium (J Jiao & Guo, 2011).

Table 2 Comparison ω(z) and$I_0(z)$ calculated in the skin tissue water medium

	$\lambda(nm)$	$I_{0s}(Z)\times 10^{8}$	$2\omega_{0R}(\mu m)$	$\omega_{zs}\left(\frac{0.001}{mm^{-1}}\right)$	$\omega_{zs}\left(\frac{0.002}{mm^{-1}}\right)$	$\omega_{zs}\left(\frac{0.003}{mm^{-1}}\right)$	$t_p(ps)$	$I_{0w}(Z)$	$\omega_{zw}\left(\frac{0.001}{mm^{-1}}\right)$	$\omega_{zw}\left(\frac{0.002}{mm^{-1}}\right)$	$\omega_{zw}\left(\frac{0.003}{mm^{-1}}\right)$
1	532	2.06	5.3	0.0000459	0.0000916	0.000137	6000	2.02×10^{8}	0.0000487	0.0000964	0.000144
2	532	4.52	3.4	0.0000719	0.000143	0.000213	30	4.51×10^{8}	0.0000756	0.000151	0.0000224
3	580	2.21	5	0.0000531	0.000106	0.000158	3	2.2×10^{8}	0.0000558	0.000111	0.000166
4	580	2.21	5	0.0000531	0.000106	0.000158	0.3	2.2×10^{8}	0.0000558	0.000111	0.000166
5	580	2.77	4.4	0.0000468	0.0000934	0.000139	0.1	2.76×10^{8}	0.0000491	0.000124	0.000147
6	1064	9.86	7.7	0.0000637	0.000127	0.000189	6000	9.69×10^{8}	0.0000639	0.000133	0.000198
7	1064	2.65	4.7	0.000104	0.000207	0.000309	30	2.6×10^{8}	0.000108	0.000218	0.000324

A USP laser system at wavelengths 532,580, 1064 nm is considered. The free-electron density was estimated in the orders of 10^{-40}–$10^{27}cm^{-3}$. We assumed average laser power is 0.065W and cylinder radius is ($r=-12.5\ldots 12.5\mu m$).

For chromophore ionization with the picoseconds and the femtosecond pulses, at all the wavelengths532, 580 and 1064 nm, from our calculations results we found that the good agreements between angle and the layer depth and the distance of focal spot. For example, according to our calculations for each medium show that maximum of generated chromophore ionization at three wavelengths for dermis layer at angles 16˚ and 22˚ is more than for epidermis layer. As expressed in (9)-(12), the multiphoton ionization rate is proportional to G^{K} and the chromophore ionization rate depends on the absorption of laser pulse energy $F(t)\mu_a$ (J Jiao & Guo, 2011). The chromophore ionization does not contribute too much to the generation of the seed electrons because of the relatively weak absorption of the chromophore (σ_a=1.85mm^{-1}) at mentioned wavelengths (J Jiao & Guo, 2011). Therefore, in the following calculationsconcerning the chromophore ionization in water medium and skin tissues induced by the picoseconds and femtosecond lasers. Figure 3 to 8, show that the variations of chromophore ionization in terms of time for water and skin tissue at certain physical condition .According to our calculations the maximum of generated chromophore ionization at the wavelength 532 nm with 6000 ps pulse duration of layer dermis angle 16˚ at the time of 2.38×10^{-8}s are 8.09×10^{33}, $3.97\times 10^{33}$for skin tissue and water, respectively.

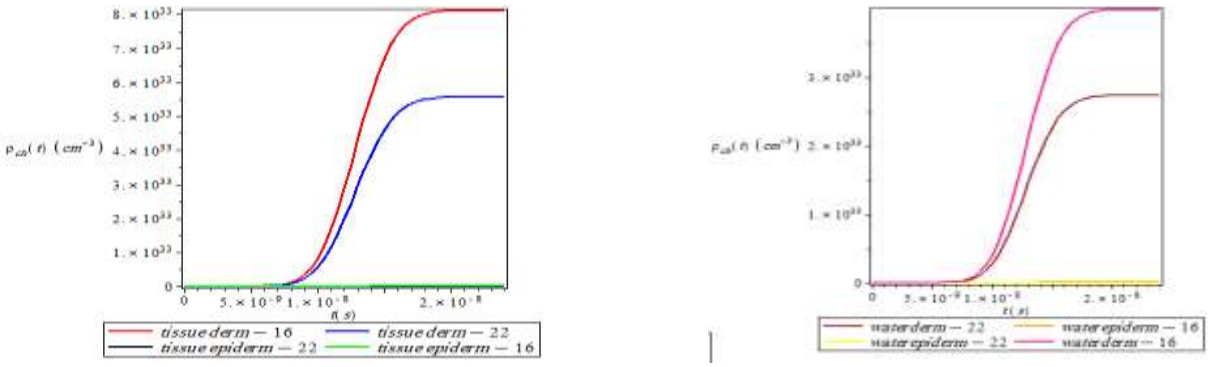

a **b**

Figure3 Comparison of the chromophore ionization as a function of the time in the wavelength 532 nm and $2\omega_{0R}=5.3\mu m$ at two angles 16˚,22˚ for dermis and epidermis layers a) Skin tissue b) Water medium

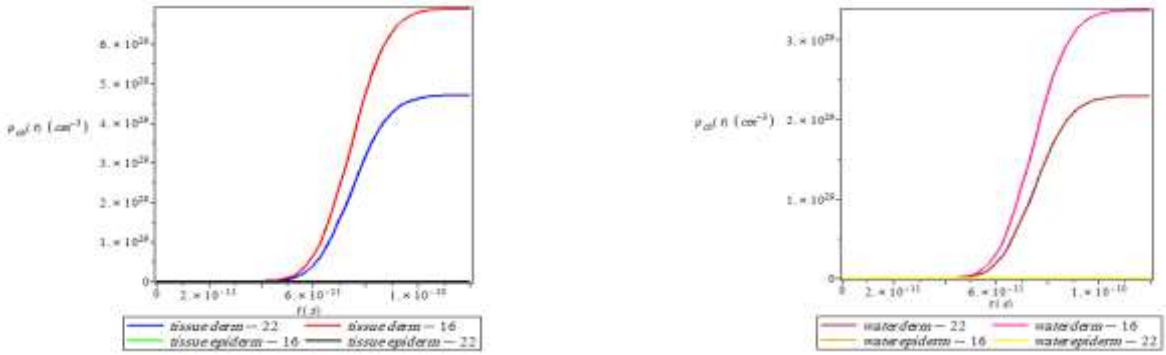

c **d**

Figure.4 Comparison of the choromophore ionization as a function of the time in the wavelength 532 nm and $2\omega_{0R}=3.4\mu m$ at two angles 16˚,22˚ for dermis and epidermis layers **c)** Skin tissue **d)** Water medium

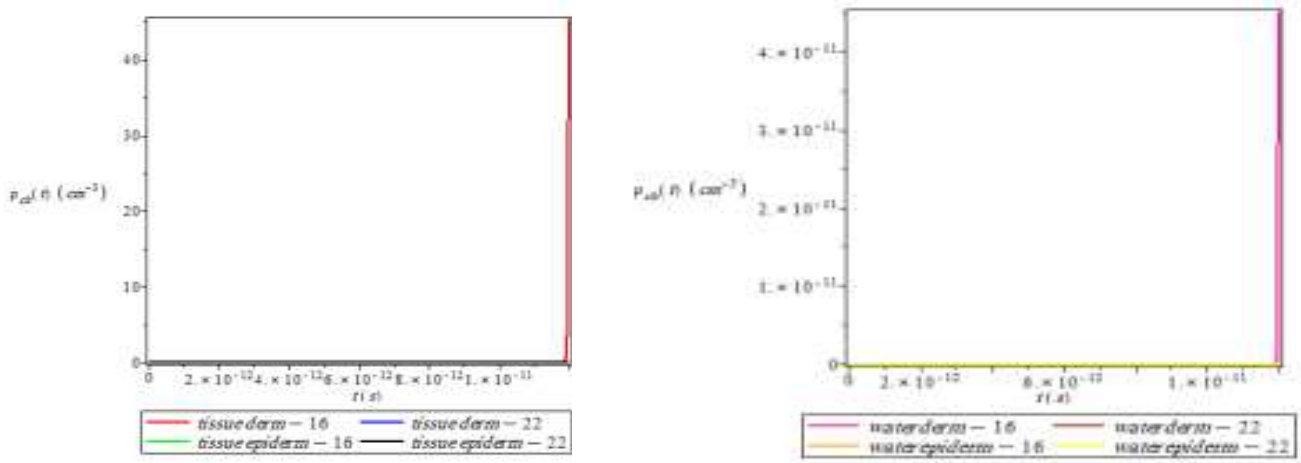

e **f**

Figure.5 Comparison of the chromophore ionization as a function of the time in the wavelength 580 nm and $2\omega_{0R} = 5\mu m$ at two angles 16˚,22˚ for dermis and epidermis layers **e)** Skin tissue **f)** Water medium

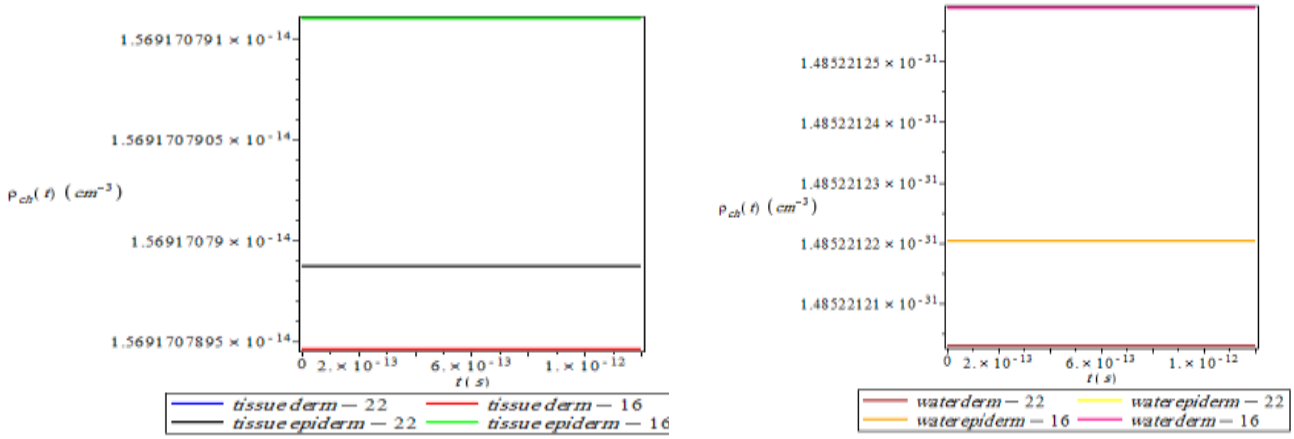

g h

Figure.6 Comparison of the chromophore ionization as a function of the time in the wavelength 580 nm and$2\omega_{0R} = 5\mu m$ and$t_p = 0.3$ psat two angles 16˚,22˚ for dermis and epidermis layers **g)** Skin tissue **h)** Water medium

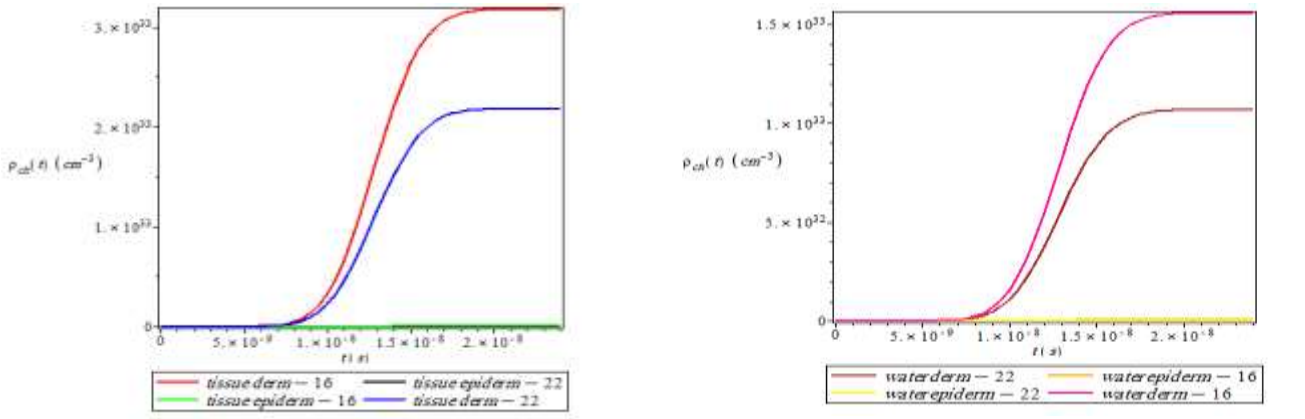

i j

Figure.7 Comparison of the chromophore ionization as a function of the time in the wavelength $1064\,nm$ and $2\omega_{0R} = 7.7\mu m$ and$t_p = 6000\,ps$ at two angles 16˚,22˚ for dermis and epidermis layers **i)** Skin tissue **j)** Water medium

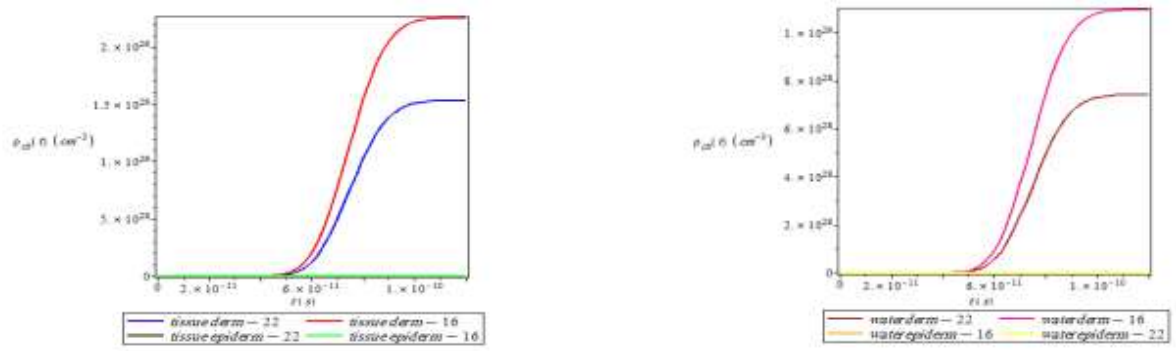

k l

Figure.8 Comparison of the chromophore ionization as a function of the time in the wavelength 1064 nm and $2\omega_{0R} = 4.7\mu m$ and$t_p = 30ps$at two angles 16˚,22˚ for dermis and epidermis layers **k)** Skin tissue **l)** Water medium

The minimum of generated chromophore ionization at the 3 ps pulse at wavelength 580 nm and angle 22˚ of epidermis layer at the time of 1.19×10^{-11} are 3.17×10^{-14}, 3.6×10^{-31} for skin tissue and water, respectively. Figure 6 shows chromophore ionization in the water medium and skin tissue with the 0.3 ps and 0.1 pulses the layers configuration with considered amount, angle, pulse duration and the time integral of the incident radiation and distance of focal spot, the first layer is dermis 16˚ and second layer is dermis 22˚, the 3rd layer is epidermis 16˚ and the last layer is epidermis 22˚. There are not differences of the viewpoint amount chromophore ionization in the layers configuration between for each medium in the 2-D and 3-D models, but from results of our calculations we found that differences are between layers configuration in the chromophore ionization with free electron density at skin tissue and water medium these differences are due to choose the Runge-Kutta algorithm and critical electron density. Also, in Figures 9 to13, we see that the two dimensional diagrams of time dependent free electron density for different wavelengths at various physical conditions for water and skin tissue media (epidermis and dermis) at choosing the incident angles 16˚ and 22˚.

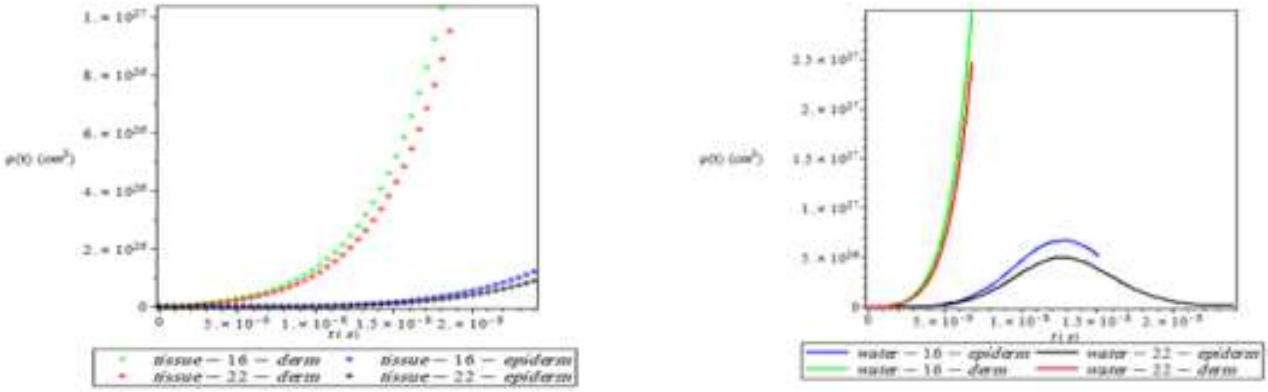

a **b**

Figure.9 Comparison of the free electron density as a function of thetime in the wavelength 532 nm and $2\omega_{0R} = 5.3\mu m$ and$t_p = 6000\ ps$at two angles 16˚,22˚ for dermis and epidermis layers **a)** Skin tissue **b)**Water medium

Table 3 Comparison of the peak spot the free electron density in the skin tissue and water medium for wavelength 532 nm with $2\omega_{0R} = 5.3\mu m$ and $t_p = 6000ps$ at two angles 16˚,22˚ for dermis and epidermis layers

Tissue type	$\rho_w(t)$	$\rho_s(t)$	$\rho_{chw}(t)$	$\rho_{chs}(t)$	$I_w^b(r,z,t)$	$I_s^b(r,z,t)$
Dermis-angle 16	2.15×10^{27}	8.25×10^{26}	3.97×10^{33}	8.09×10^{33}	٦١١٨٠,٢٥	٦٨٠٦٣,١٢
Epidermis-angle16	6.72×10^{26}	1.22×10^{26}	5.28×10^{30}	1.08×10^{31}	١٨٥٣,٠٣	٢٠٦٩,٠٢
Dermis-angle22	2.45×10^{27}	7.46×10^{26}	2.73×10^{33}	5.55×10^{33}	٤٧٧٦٠,٦٩	٥٢٩٨١,٤٩
epidermis-angle22	4.97×10^{26}	9.09×10^{25}	2.88×10^{30}	5.91×10^{30}	١٢٣٨,٦٧	١٣٨٧,٦٥

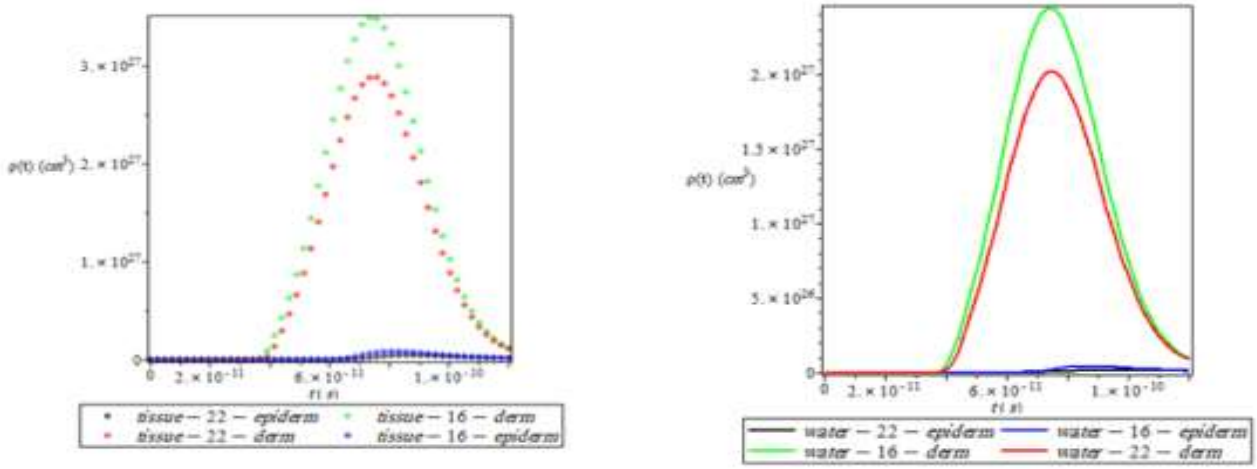

c **d**

Figure.10 Comparison of the free electron density as a function of the time in the wavelength 532 nm and $2\omega_{0R} = 3.4\mu m$ and$t_p = 30ps$ at two angles 16˚,22˚ for dermis and epidermis layers **c)** Skin tissue **d)**Water medium

Table 4 Comparison of the peak spot the free electron density in the skin tissue and water medium for wavelength 532 nm with $2\omega_{0R} = 3.4\mu m$ and $t_p = 30ps$at two angles 16˚,22˚ for dermis and epidermis layers

Tissue type	$\rho_w(t)$	$\rho_s(t)$	$\rho_{chw}(t)$	$\rho_{chs}(t)$	$I_w^b(r,z,t)$	$I_s^b(r,z,t)$
Dermis-angle 16	2.45×10^{27}	3.48×10^{27}	3.36×10^{29}	6.68×10^{29}	٦١١٨٢,٢٥	٢٦٤٦٤,٤
epidermis-angle16	3.73×10^{25}	8.75×10^{25}	1.06×10^{26}	3.67×10^{26}	١٨٥٣,٠٩	٧٧٢,٥
Dermis-angle22	2.01×10^{27}	2.87×10^{27}	2.29×10^{29}	4.68×10^{29}	٤٧٤٦٣,٧٣	٢٠٤٧٥,٩٦
epidermis-angle22	1.43×10^{25}	4.85×10^{25}	2.88×10^{25}	1.3×10^{26}	١٢٣٨,٦٨	٥١٤,٠٧

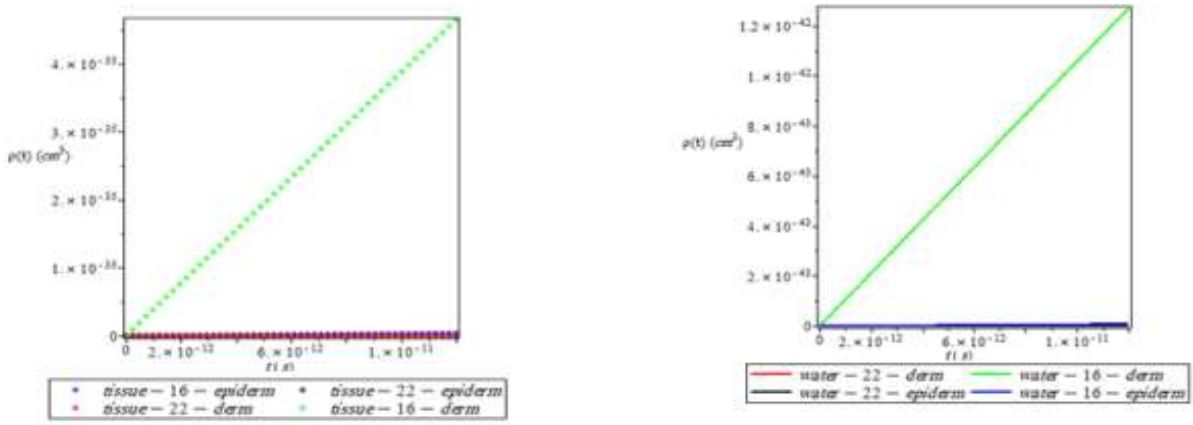

e **f**

Figure.11 Comparison of the free electron density as a function of the time in the wavelength 580 nm and $2\omega_{0R} = 5\mu m$ and $t_p = 3ps$ at two angles 16˚,22˚ for dermis and epidermis layers **e)** Skin tissue **f)**Watermedium

Table 5 Comparison of the peak spot the free electron density in the skin tissue and water medium for wavelength 580 nm with $2\omega_{0R} = 5\mu m$, $t_p = 3ps$at two angles 16˚,22˚ for dermis and epidermis layers

Tissue type	$\rho_w(t)$	$\rho_s(t)$	$\rho_{chw}(t)$	$\rho_{chs}(t)$	$I_w^b(r,z,t)$	$I_s^b(r,z,t)$
Dermis-angle 16	4.59×10^{-24}	4.46×10^{-35}	4.5×10^{-11}	45.2	168.87	١٩١,٢٥
epidermis-angle16	2.71×10^{-26}	4.32×10^{-37}	3.6×10^{-31}	3.17×10^{-14}	٥,٠٥٤	٥,٧٤١
Dermis-angle22	4.11×10^{-27}	7.92×10^{-35}	1.5×10^{25}	7.9×10^{-10}	٣٨,٤٢	٤٣,٦٧
epidermis-angle22	1.8×10^{-29}	6×10^{-40}	1.74×10^{-31}	1.78×10^{26}	٠,٩٨٤	١,١٢٥

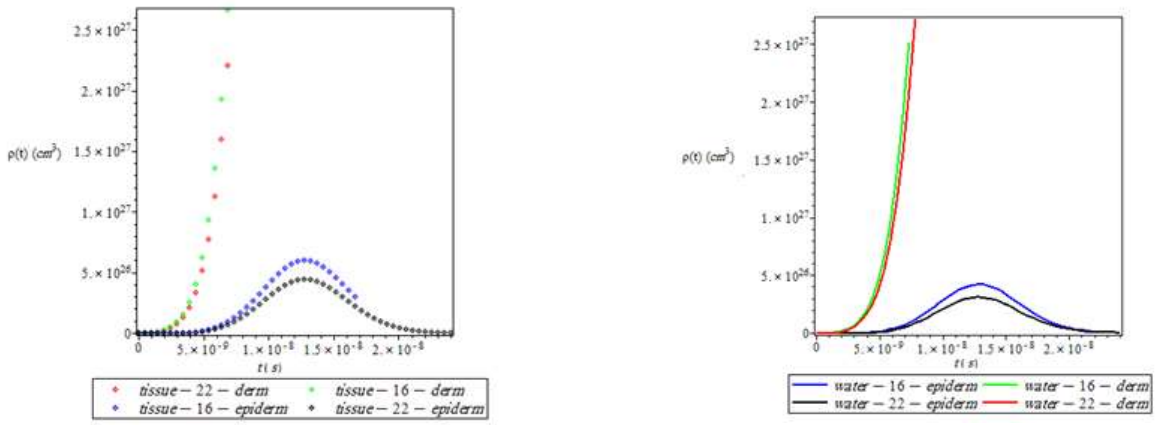

i j

Figure.12 Comparison of the free electron density as a function of the time in the wavelength1064 nm and $2\omega_{0R} = 7.7\mu m$ and $t_p = 6000ps$ at two angles 16˚,22˚ for dermis and epidermis layers **i)** Skin tissue **j)** Water medium

Table 6 Comparison of the peak spot the free electron density in the skin tissue and water medium for wavelength 1064 nm with $2\omega_{0R} = 7.7\mu m$ and $t_p = 6000ps$at two angles 16˚, 22˚ for dermis and epidermis layers

Tissue type	$\rho_w(t)$	$\rho_s(t)$	$\rho_{chw}(t)$	$\rho_{chs}(t)$	$I_w^b(r,z,t)$	$I_s^b(r,z,t)$
Dermis-angle 16	1.85×10^{27}	1.92×10^{27}	1.55×10^{33}	3.17×10^{33}	٣٢٧٠٧,٣٦	٣٦٥٤٠,٠٥
epidermis-angle16	4.21×10^{26}	6.1×10^{26}	2.07×10^{30}	4.26×10^{30}	٩٩٤,٢٤	١١١١,٥٤
Dermis-angle22	2.06×10^{27}	2.2×10^{27}	1.07×10^{33}	2.18×10^{33}	٢٥٥٣٩,٨٥	٢٨٣٦٢,٥٤
epidermis-angle22	3.11×10^{26}	4.54×10^{26}	1.13×10^{33}	2.33×10^{30}	٦٦٤,٨٨	٧٤٣,٤٩

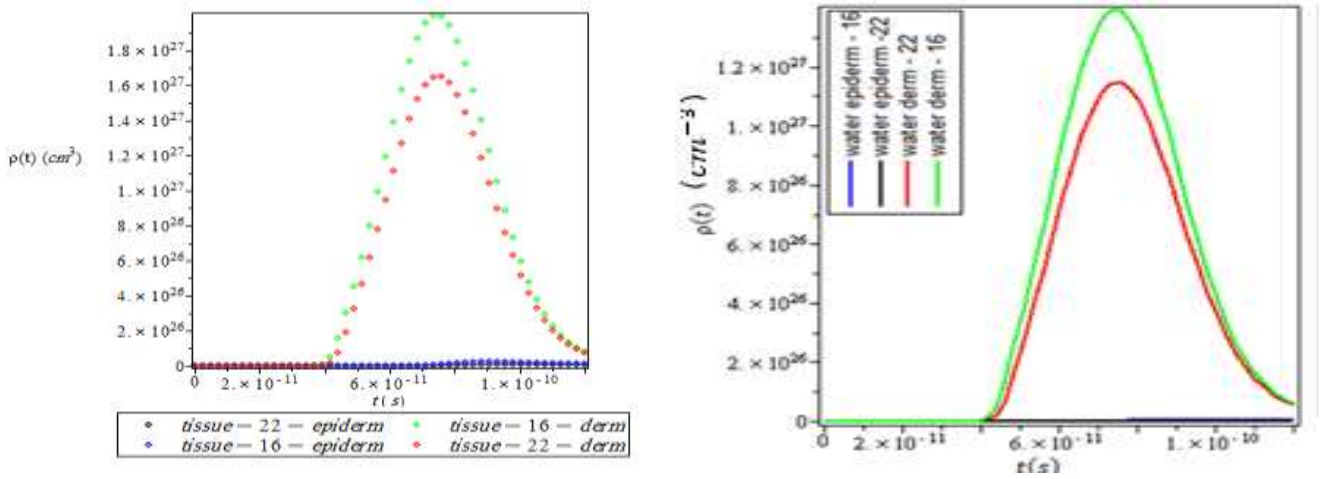

k l

Figure.13 Comparison of the free electron density as a function of the time in the wavelength1064 nm and $2\omega_{0R} = 4.7\mu m$ and $t_p = 30ps$ at two angles 16˚,22˚ for dermis and epidermis layers **k)** Skin tissue **l)** Watermedium

Table 7 Comparison of the peak spot the free electron density in the skin tissue and water medium for wavelength 1064 nm with $2\omega_{0R} = 4.7\mu m$ and $t_p = 30ps$ at two angles 16˚,22˚ for dermis and epidermis layers.

Tissue type	$\rho_w(t)$	$\rho_s(t)$	$\rho_{chw}(t)$	$\rho_{chs}(t)$	$I_w^b(r,z,t)$	$I_s^b(r,z,t)$
Dermis-angle 16	1.39×10^{27}	1.99×10^{27}	1.09×10^{29}	2.25×10^{29}	١١٤٠٥,٣٥	١٢٦٦٢,٧
epidermis-angle16	4.87×10^{24}	2.57×10^{25}	7.84×10^{24}	4.78×10^{25}	٣٣١,٩٩	٣٦٩,١٣
Dermis-angle22	1.14×10^{27}	1.65×10^{27}	7.39×10^{28}	1.53×10^{29}	٨٨٥٠,٥٩	٩٨٢٦,٤٣
epidermis-angle22	7.1×10^{23}	8.36×10^{24}	1.04×10^{24}	1.08×10^{25}	٢٢٠,٢١	٢٤٥,٤٣

In tables 3 to 7, our calculations results of numerical values of intensity radiation laser, chromophore ionization and time dependent free electron density for various wavelengths at different physical conditions at two angles 16˚ and 22˚ for two layers (epidermis and dermis) for water and skin tissue. By seeing the Table 3 to 7, we will find that the good agreement is seen between free electron density and critical electron density and layers configuration with considered wavelengths and pulse durations.

Time dependent free electron density for two wavelengths of 1064 nm, 532 nm with 6 ns pulse duration is the slight difference with the other wavelengths at various physical conditions from the point view of layers configuration. This difference is due to critical free electron density, there for, according to our calculations, the maximum of generated free electron density at wavelength1064 nm with 6 ns pulse duration at the dermis layer of skin tissue are 2.2×10^{27}, 1.92×10^{27} for angle 22˚and 16˚, respectively and for the maximum of generated free electron density at the dermis layer of water medium are 2.06×10^{27}, 1.85×10^{27} for angle 22˚and 16˚, respectively.

According to our calculations the critical free electron density in water medium at the wavelengths 532 nm and 1064 nm of layer dermis 22˚ are 7.67×10^{24}, 6.45×10^{24}, and for layer dermis 16˚ are 6.7×10^{24}, 5.79×10^{24}, respectively. Our computations show that for ablation in skin tissue and water media at 580 nm wavelength with two pulse duration 0.1 ps and 0.3 ps the time dependent free electron density is about 0. This is duo to very short pulse duration and $I^b \cong 0$ .Our calculations show that free electron density and chromophore ionization is increasing with increasing time and the time dependent integral of the incident radiation and the radiation intensity.

For ablation with the picosecond and femtosecond pulses, at all the wavelength 532, 580 and 1064 nm, from calculations results we conclude that the good agreement between layers configuration with considering angle and the distance of spot focal. Therefore from table 3 to 7 we see that concerning the ablation in water medium and skin tissue induced by the picosecond and femtosecond lasers, maximum free electron density for wavelength 532 nm with 6 ns pulse duration of dermis layer at angle 16˚ are 3.48×10^{27}in the time7.25×10^{-11} and 2.45×10^{27} in the time 7.43×10^{-11} for skin tissue and water, respectively. Therefore , according to our calculations the minimum of generated free electron density of epidermis 22˚ at 3 ps pulse and 580 nm wavelength at the time of $1.19\times 10^{-11}$are 6×10^{-40},1.8×10^{-29} for skin tissue and water, respectively. From fig (9)-(13) we see that the free electron density could expand initially of the occurrence of cascade ionization with more laser energy.

Focused laser beam was incident on the surface of the epidermis or inside the skin tissue or the water medium. A USP laser system at wavelength 1064nm with 30 ps pulse duration is considered. The critical free-electron density would be estimated in the order of $10^{21}-10^{25}cm^{-3}$.

A good agreement is found between numerical models the presented results from the layer epidermis in the water medium at the wavelength 1064 nm for angle 22 degree.

To remove the cancerous cells exiting in the skin layers effectively, a laser beam can be focused inside the skin and water to the dermis angle 16 degree surface. The critical electron density epidermis layer is small therefore, the free electron density is a very small a dermis layer.

CONCLUSIONS

In this work, our studies are established on the ultra short pulsed laser on the skin tissue and water in cylindrical coordinates. The temporal evolutions of the free-electron density are calculated using numerical methods (fourth-order Runge-Kutta). A parametric study with regarding to the free electron density (plasma) in the skin tissue and water medium on the dermis and epidermis layers at angle 16 and 22 degree are concluded.

In this work, a 2-D and 3-D models are established in combining the chromophore ionization rate and the I^b to investigate the temporal evolutions of the free-electron density in skin tissues and water. From our obtained results we found that the good agreement between layers configuration with considering angle, the extinction coefficient, layers depth and the distance of spot focal. Our studies on this work, show that if the amount of radiation intensity of pulsed laser is increased and the distance of focal spot is decreased the amount of time dependent free-electron density more and more, such that this case is proper for skin cancer treatment.

Also, our calculations for each medium (water and skin tissue) show that optimum time dependent free electron density, I^b and the chromophore ionization rate for dermis layer at angle 16˚ and 22˚ are functions of wavelength, beam width, beam radius, amplitude of the beam radiation strength. Also pulse duration is more than for epidermis layer. Here we concludefree electron density produced by skin tissue is more than of water medium at the wavelengths 532 nm with $2\omega_{0R}=5.3\mu m$ and 580 with$t_p=3ps$.

Our calculations show that free electron density and chromophore ionization is increasing with increasing time and the time integral of the incident radiation and the radiation intensity. From calculations results we found that the good agreement between layers configuration of viewpoint amount for the free electron density rate equation and chromophore ionization with considering angle and distance of focal spot and I^b . The first layer is dermis with angle 16 degree, latter layer is dermis with 22 degree, the 3rd layer is epidermis 16 degree and the last layer is epidermis 22 degree.

At the epidermis layer 22 degree, the free electron density is very small. The influence of various ionization mechanism including, chromophore ionization pathways on the process of plasma generation for the model skin tissue and water medium is investigated. A good agreement is found between layers configuration in 2-D and 3-D models of choromophore ionization in water medium and skin tissue but the slight differences are between layers configuration in chromophore ionization with free electron density at skin tissue and water medium can due to differences in the Runge-Kutta algorithm and critical electron density.

REFERENCE

Ding, H., Lu, J. Q., Wooden, W. A., Kragel, P. J., & Hu, X.-H. (2006). Refractive indices of human skin tissues at eight wavelengths and estimated dispersion relations between 300 and 1600 nm. *Physics in medicine and biology*, *51*(6), 1479.

Docchio, F., Regondi, P., Capon, M. R., & Mellerio, J. (1988). Study of the temporal and spatial dynamics of plasmas induced in liquids by nanosecond Nd: YAG laser pulses. 1: Analysis of the plasma starting times. *Applied optics*, *27*(17), 3661-3668.

Fan, C. H., and Longtin, J. P. (2003). Radiative energy transport at the spatial and temporal mi-cro/nanoscales *Radiative energy transport at the spatial and temporal mi-cro/nanoscales*. UK: WITPress, Southampton, UK.

Fang, Q., & Hu, X.-H. (2004). Modeling of skin tissue ablation by nanosecond pulses from ultraviolet to near-infrared and comparison with experimental results. *Quantum Electronics, IEEE Journal of*, *40*(1), 69-77.

Guo, Z., & Kumar, S. (2002). Three-dimensional discrete ordinates method in transient radiative transfer. *Journal of thermophysics and heat transfer*, *16*(3), 289-296.

Guo, Z., Kumar, S., & San, K.-C. (2000). Multidimensional Monte Carlo simulation of short-pulse laser transport in scattering media. *Journal of thermophysics and heat transfer*, *14*(4), 504-511.

Huang, H., & Guo, Z. (2010). Ultrashort pulsed laser ablation and stripping of freeze-dried dermis. *Lasers in medical science*, *25*(4), 517-524.

Huang, K., Guo, J., & Xu, Z. (2009). Recycling of waste printed circuit boards: A review of current technologies and treatment status in China. *Journal of Hazardous Materials*, *164*(2), 399-408.

Jiao, J. (2011). *Simulation of laser-tissue thermal interaction and plasma-mediated ablation.* Rutgers University-Graduate School-New Brunswick.

Jiao, J., & Guo, Z. (2009). Thermal interaction of short-pulsed laser focused beams with skin tissues. *Physics in medicine and biology*, *54*(13), 4225.

Jiao, J., & Guo, Z. (2011). Modeling of ultrashort pulsed laser ablation in water and biological tissues in cylindrical coordinates. *Applied Physics B*, *103*(1), 195-205.

Kennedy, P. K. (1995). A first-order model for computation of laser-induced breakdown thresholds in ocular and aqueous media. I. Theory. *Quantum Electronics, IEEE Journal of*, *31*(12), 2241-2249.

Kim, K., & Guo, Z. (2004). Ultrafast radiation heat transfer in laser tissue welding and soldering. *Numerical Heat Transfer, Part A: Applications*, *46*(1), 23-40.

Kumar, Z. G., Sunil. (2001). Radiation element method for transient hyperbolic radiative transfer in plane-parallel inhomogeneous media. *Numerical Heat Transfer: Part B: Fundamentals*, *39*(4), 371-387.

Mester, E., Spiry, T., Szende, B., & Tota, J. G. (1971). Effect of laser rays on wound healing. *The American Journal of Surgery*, *122*(4), 532-535.

Nieto, D., Flores-Arias, M. T., O'Connor, G. M., & Gómez-Reino, C. (2011). *Fabrication of microlens arrays on soda-lima glasses with a Nd: YVO4laser.* Paper presented at the International Conference on Applications of Optics and Photonics.

Tata, D. B., & Waynant, R. W. (2011). Laser therapy: A review of its mechanism of action and potential medical applications. *Laser & Photonics Reviews*, *5*(1), 1-12.

Williams, F., Varma, S., & Hillenius, S. (2008). Liquid water as a lone-pair amorphous semiconductor. *The Journal of Chemical Physics*, *64*(4), 1549-1554.

Zhou, J., Chen, J., & Zhang, Y. (2008). Numerical modeling of transient progression of plasma formation in biological tissues induced by short laser pulses. *Applied Physics B*, *90*(1), 141-148.

